

The additionality problem of Ocean Alkalinity Enhancement

Lennart T. Bach

Institute for Marine and Antarctic Studies, University of Tasmania, Hobart, TAS, Australia.

Correspondence to: Lennart T. Bach (Lennart.bach@utas.edu.au)

Abstract. Ocean Alkalinity Enhancement (OAE) is an emerging approach for atmospheric carbon dioxide removal (CDR). The net climatic benefit of OAE depends on how much it can increase CO₂ sequestration relative to a baseline state without OAE. This so-called ‘additionality’ can be calculated as:

$$\text{Additionality} = C_{\text{OAE}} - \Delta C_{\text{baseline}}$$

So far, feasibility studies on OAE have mainly focussed on enhancing alkalinity in the oceans to stimulate CO₂ sequestration (C_{OAE}) but not primarily how such anthropogenic alkalinity would modify the natural alkalinity cycle and associated baseline CO₂ sequestration ($\Delta C_{\text{baseline}}$). Here, I present incubation experiments where materials considered for OAE (sodium hydroxide, steel slag, olivine) are exposed to beach sand to investigate the influence of anthropogenic alkalinity on natural alkalinity sources and sinks. The experiments show that anthropogenic alkalinity can strongly reduce the generation of natural alkalinity, thereby reducing additionality. This is because the anthropogenic alkalinity increases the calcium carbonate saturation state, which reduces the dissolution of calcium carbonate from sand, a natural alkalinity source. I argue that this ‘additionality problem’ of OAE is potentially widespread and applies to many marine systems where OAE implementation is considered – far beyond the beach scenario investigated in this study. However, the problem can potentially be mitigated by dilute dosing of anthropogenic alkalinity into the ocean environment, and avoid OAE at hotspots of natural alkalinity cycling such as in marine sediments. Understanding a potential slowdown of the natural alkalinity cycle through the introduction of an anthropogenic alkalinity cycle will be crucial for the assessment of OAE.

1. Introduction

Keeping global warming between 1.5 to 2°C requires rapid reduction of greenhouse gas emissions and gigatonne-scale atmospheric carbon dioxide removal (CDR), using a portfolio of terrestrial and marine CDR methods (Nemet et al., 2018) Ocean alkalinity enhancement (OAE) is considered as an important

CDR method of the marine portfolio (Hartmann et al., 2013). OAE can be achieved through a variety of geochemical and electrochemical processes (Renforth and Henderson, 2017). All of them enhance surface ocean alkalinity to reduce the hydrogen ion (H^+) concentration in seawater (i.e. increase pH). This reduction in $[H^+]$ causes a shift in the carbonate chemistry equilibrium:



from CO_2 on the left towards bicarbonate (HCO_3^-) and carbonate ion (CO_3^{2-}) on the right. The associated reduction of the CO_2 partial pressure in seawater (pCO_2) enables atmospheric CO_2 influx into the oceans (or reduces CO_2 outflux if $pCO_2 > \text{atmospheric } pCO_2$). This transfer (retention) of atmospheric CO_2 into the ocean leads to an increase of the dissolved inorganic carbon (DIC) concentration in seawater, with DIC defined as:

$$DIC = [CO_2] + [HCO_3^-] + [CO_3^{2-}] \quad (2)$$

Among the widely discussed OAE approaches are coastal enhanced weathering and electrodialytical acid removal (Eisaman et al., 2023). Coastal enhanced weathering achieves alkalinity increase via the addition of pulverized alkaline rocks like limestone, olivine, or alkaline industrial products like steel slag to coastal environments (Meysman and Montserrat, 2017; Feng et al., 2017; Harvey, 2008; Schuiling and Krijgsman, 2006; Renforth, 2019).

Electrodialytical OAE is somewhat different from coastal enhanced weathering since no materials are added to seawater. Instead, water dissociation into H^+ and OH^- is catalyzed in bipolar membranes, and these ions are then separated using electrical energy and ion-selective membranes (de Lannoy et al., 2018). H^+ is captured as hydrochloric acid whilst OH^- is captured as sodium hydroxide (NaOH). The hydrochloric acid needs to be utilised, neutralized in deep ocean sediments, or stored in save reservoirs outside the ocean (Eisaman et al., 2018; Tyka et al., 2022). NaOH is enriched in the processed seawater, which is released back into the surface to convert CO_2 into HCO_3^- (Eisaman et al., 2018; Tyka et al., 2022).

A critical side-effect of OAE is the associated increase in CO_3^{2-} concentrations, which comes through the shift in the marine carbonate equilibrium through H^+ absorption (see above). This increase elevates the saturation state for calcium carbonate (Ω_{CaCO_3}), the metric which determines the solubility of $CaCO_3$ in seawater. Ω_{CaCO_3} is defined as:

$$\Omega_{CaCO_3} = \frac{[Ca^{2+}]_{sw} \times [CO_3^{2-}]_{sw}}{K_{sp}} \quad (3)$$

where $[Ca^{2+}]_{sw}$ and $[CO_3^{2-}]_{sw}$ are calcium ion (Ca^{2+}) and CO_3^{2-} concentration in seawater and K_{sp} is the empirically determined solubility product (Mucci, 1983). K_{sp} differs for different crystal forms of $CaCO_3$. It is higher for Aragonite than for Calcite, meaning Aragonite is more soluble (Mucci, 1983). Aragonite (Arg) and Calcite (Cal) precipitation is thermodynamically favoured when Ω_{Arg} and Ω_{Cal} are ≥ 1 (Adkins et al., 2020). $CaCO_3$ precipitation is of high relevance for the assessment of OAE as the drawdown of CO_3^{2-} through precipitation reduces alkalinity, shifts the carbonate chemistry equilibrium (eq. 1) towards CO_2 and thus counters the CDR efficiency of OAE (Moras et al., 2022; Fuhr et al., 2022; Hartmann et al., 2023).

Logistical constraints suggest that OAE would at least initially more likely to be conducted in coastal environments (Renforth and Henderson, 2017; Lezaun, 2021; He and Tyka, 2023). Here, alkalinity-enhanced seawater would likely be in contact with marine sediments (Meysman and Montserrat, 2017; Feng et al., 2017; Harvey, 2008). The highly abundant particles in marine sediments can serve as nuclei for $CaCO_3$ precipitation thereby catalysing alkalinity loss when Ω_{CaCO_3} is ≥ 1 (Zhong and Mucci, 1989; Morse et al., 2003; Adkins et al., 2020). This constitutes a problem for OAE because alkalinity-enhanced seawater with its high Ω_{CaCO_3} is then exposed to particles that catalyse precipitation. Indeed, recent studies have demonstrated that this particle-catalysed precipitation can rapidly reduce alkalinity, with the degree and rate of alkalinity reduction depending on the amount of alkalinity added and the particle concentrations (Moras et al., 2022; Fuhr et al., 2022; Hartmann et al., 2023).

Particle-catalysed $CaCO_3$ precipitation has received significant consideration as a loss term for OAE efficiency (Renforth and Henderson, 2017; Moras et al., 2022; Fuhr et al., 2022; Hartmann et al., 2013, 2023). However, there is another complication affecting OAE efficiency near sediments, which has received no attention and will be in focus of this study. Sediments can not only provide precipitation nuclei but also constitute natural alkalinity sources, for example via dissolution of $CaCO_3$ or other carbonates (Torres et al., 2020; Wallmann et al., 2022; Krumins et al., 2013; Aller, 1982; Middelburg et al., 2020). Sandy beaches can be rich in biogenic carbonates and organic matter thereby creating environments of high respiratory CO_2 . Accordingly, Ω_{CaCO_3} is low close to the sediments or within pore waters and $CaCO_3$ dissolution is favoured (Liu et al., 2021; Perkins et al., 2022; Reckhardt et al., 2015). This form of natural alkalinity formation via $CaCO_3$ dissolution can sequester CO_2 which may have otherwise be released into the atmosphere (Saderne et al., 2021; Krumins et al., 2013; Aller, 1982; Fakhraee et al., 2023; Archer et al., 1998). OAE within these naturally low Ω_{CaCO_3} environments could have two effects. First, it would have the desired effect of consuming H^+ and increasing CO_2 sequestration via the generation of anthropogenic alkalinity. Second, the consumption of H^+ would increase Ω_{CaCO_3} , which could reduce the dissolution of $CaCO_3$ and thus reduce natural CO_2 sequestration since less natural alkalinity is produced. Due to this second effect, the first (desired) effect of CO_2 sequestration may be significantly reduced. Accordingly, the net gain in CO_2 sequestration would be lower than one would have hoped for.

The concept “additionality” describes the net gain in CO₂ sequestration achieved through the implementation of a CDR method relative to a hypothetical baseline (or “business-as-usual”) scenario (Michaelowa et al., 2019). Per definition, “additional” is all CO₂ sequestration achieved through the implementation of a CDR method (here OAE) that goes beyond natural and anthropogenic CO₂ sequestration that already occurs in the baseline scenario without the implementation of the CDR method. Additionality is a central concept in climate policy that has been utilized for carbon accounting in the Clean Development Mechanism established under the 1997 Kyoto Protocol (Havukainen et al., 2022). It can be defined in simple terms as:

$$\text{Additionality} = C_{\text{OAE}} - \Delta C_{\text{baseline}} \quad (4)$$

where C_{OAE} is the CO₂ sequestration achieved through OAE, and $\Delta C_{\text{baseline}}$ is the change in the baseline CO₂ sequestration through the implementation of OAE.

This study aims to reveal and describe how anthropogenic alkalinity affects natural alkalinity release to better understand the CO₂ sequestration potential of OAE in the context of additionality. I present observational data and three experiments where three types of anthropogenic alkalinity sources (NaOH, steel slag, olivine) are exposed to a natural alkalinity source and sink (beach sand) to investigate their interactions. Afterwards, I examine these interactions (termed “additionality problem”), discuss their relevance, and how it could be managed.

2. Methods

2.1. Carbonate chemistry and dissolved silicate transects along Southern Tasmanian beaches

The project was initialised with near-shore alkalinity, pH, and dissolved silicate (Si(OH)₄) transects on four Tasmanian beaches to determine whether these beaches are detectable alkalinity sinks or sources. The investigated beaches were Clifton South, Clifton North, Goats, and Wedge on the Southarm near Hobart (Tasmania; Fig. 1, Table S1).

Samples for alkalinity and Si(OH)₄ were taken by filling 200 mL seawater from 0.2 m depth into a polyethylene (PE) bottle. Samples for pH were collected in a 60 mL polystyrene (PS) jars filled and closed at 0.2 m depth. Both the PE bottles and the PS jars were pre-rinsed with sample. The sample closest to shore was taken in the swash zone (zone where wave bores run up and down the beach) at the spot where a wave bore reached highest within ~5 minutes of observation. A ~0.2 m deep hole was dug (Fig. 1) and water was collected from the groundwater with a 60 mL syringe. The second sample was from the upper part of the swash zone where waves pushed water up the beach. Samples further out were taken from within the wave breaking zone to about 50-100 m beyond the wave breaking zone.

Samples were taken by walking into the water to the point it became too deep and a surfboard was used as sampling vehicle.

The samples were transported back to the beach where pH was measured within 15 minutes after sampling as described in section 2.4. Alkalinity and Si(OH)_4 samples were filtered after pH measurements with a 0.22 syringe filter (nylon membrane) into a 125 mL PE bottle (alkalinity) or 60 mL PS plastic jar (Si(OH)_4). Both containers, the syringe, and the syringe filter were pre-rinsed with sample.

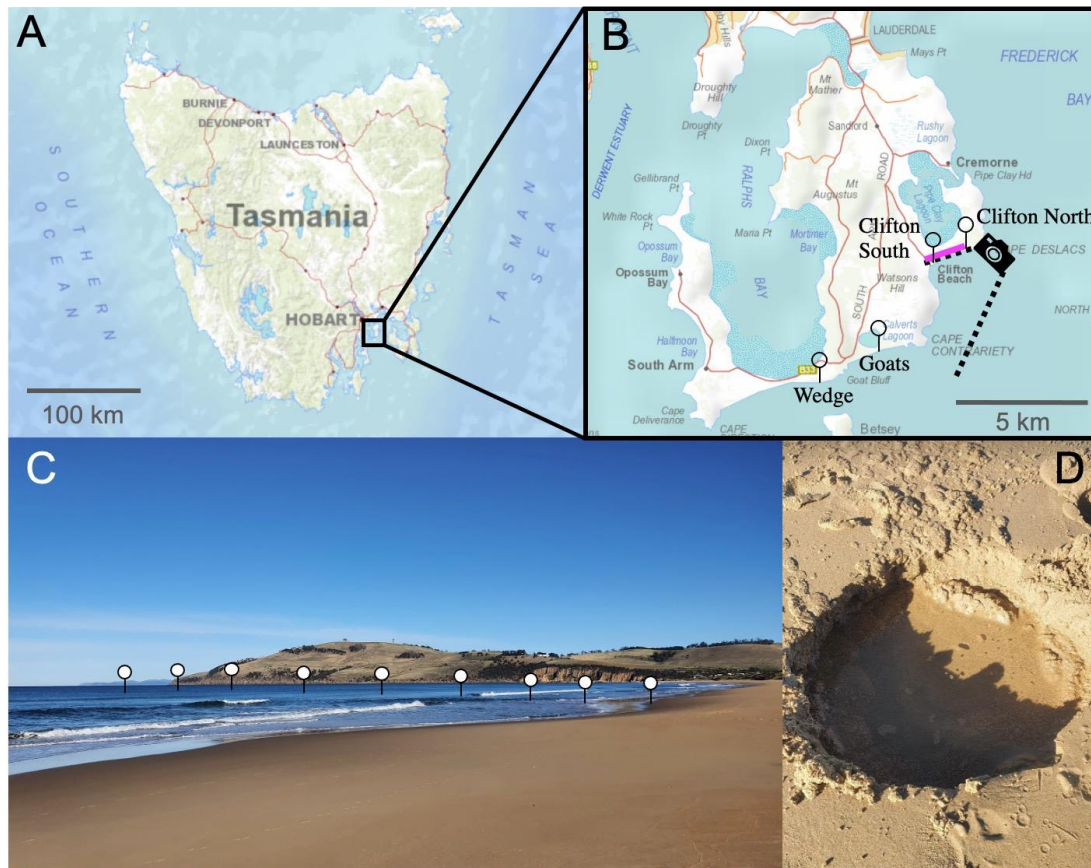


Figure 1. Locations of the beach transects and beach sand sampling in Tasmania. (A) Map of Tasmania with (B) enlarged map of the Southarm region south of Hobart. Needles show locations the beach transects and the pink line along Clifton Beach shows where sand samples (Sand 1-5) were collected for incubation experiments. The camera symbol illustrates the position from where the picture shown in panel (C) was taken. (C) illustrates approximate location of one of the beach transects. (D) A hole that was dug to sample seawater just above the swash zone, i.e. the first sample location along the transects from the beach towards 150-200 m offshore. The maps were reproduced with the permission of the Environment Heritage and Land Division, Department of Natural Resources and Environment Tasmania, © State of Tasmania.

2.2. Laboratory experiments

2.2.1. Experiment 1: Replicated dissolution assays to monitor interaction between beach sand and alkaline materials

Experiment 1 was designed to investigate the interaction between 4 different beach sands and alkaline materials during the incubation in seawater. The experiment required 60 HDPE bottles, each with a volume of 125 mL. These 60 bottles were thoroughly cleaned with double-deionised water and dried at 60°C. Twelve bottles were filled with sand from one of the 4 sampling locations (section 2.3.), respectively (totalling 48 bottles). Another set of 12 bottles were not filled with sand. This yielded 5 sets of 12 bottles (Fig. 2). Of each set, 3 bottles remained without further addition, 3 received 51.3 µL of 1 molar NaOH (targeted alkalinity increase was 428 µmol/kg), 3 received 0.0065 g of ground steel slag, and 3 received 1 g of ground olivine (Fig. 2; sand, steel slag, and olivine properties were determined as described in section 2.3.). The 48 bottles that contained sand were filled with 10 g of sand if slag or NaOH was added or 9 g of sand if olivine was added. This was done so that the weights of added sand plus alkalinity feedstock was always ~10 g.

Once the solid components were added, each bottle was filled with 120 (+/-4) g of seawater (Salinity = 35 ±0.2, alkalinity = 2259.7 µmol/kg) collected in July 2022 in the Derwent Estuary near Taroona. Salinity and pH of the seawater was determined a few minutes before transfer into the incubation bottles with a Metrohm 914 pH/conductivity meter as described in section 2.4. The transfer of the seawater into the incubation bottles took 30 minutes in total (please note that in the case of NaOH additions, seawater was added to the bottles before 51.3 µL of 1 molar NaOH was added). The incubation bottles were immediately mounted on a plankton wheel (1.06 m diameter, 2 rounds per minute), which was placed in a temperature-controlled room set to 15°C (Fig. S1). The plankton wheel kept the various mixtures of sand, alkalinity source, and seawater moving inside the bottles. The experiment commenced at 16:00 on the 17th of August, 2022.

After ~6.8 days (24th of August), bottles were consecutively removed from the plankton wheel in random order between 8:00 and 15:30. pH was measured inside the bottle with a pH electrode, directly after a bottle was taken off the plankton wheel. Afterwards, the alkalinity sample was filtered with a syringe through a 0.2 µm nylon filter into a dry and clean 125 mL HDPE bottle and stored in the dark at 7°C.

2.2.2. Experiment 2: Alkalinity formation at Omega gradients

Experiment 2 was designed to investigate whether a decline of Ω_{CaCO_3} enhances the formation of natural alkalinity via CaCO_3 dissolution and how anthropogenic alkalinity sources (olivine, slag, NaOH) influence this process. The experiment required 60 HDPE bottles (125 mL) cleaned with acid and double-deionised water (note that acid was used in Experiment 2 to make sure all remnants from Experiment 1 were washed out of the bottles). All 60 incubation bottles were filled with sand from

Clifton Beach (section 2.4.). The treatments were then set up as follows: Twelve bottles were filled only with 10 g of sand; Twelve with 10 g of sand and 0.006515 (± 0.00007) g steel slag; Twelve with 9 g of sand and 1 (± 0.002) g of olivine; Eight with 10 g of sand at “un-equilibrated” NaOH addition; Sixteen with 10 g of sand at “equilibrated” NaOH addition (Fig. 2).

For each treatment, a gradient in seawater CO₂ concentrations was established from bottle 1 (lowest CO₂) to bottle 8-16 (highest CO₂). This was achieved with the following approach: A batch of seawater (Salinity= 35 ± 0.2 , alkalinity = $2266.8 \mu\text{mol/kg}$) was collected in November 2022 in the Derwent Estuary near Taroona. About 0.3L of the batch was bubbled with pure CO₂ gas for about 5 minutes to generate highly CO₂-enriched seawater. Another ~7L of the batch was used as source water to fill the incubation bottles. pH and temperature were measured in this batch prior to filling the incubation bottles. The low CO₂ incubation bottles (bottle 1 in the sequence from e.g. 1 to 12, Fig. 2) were then filled first. Afterwards, about 20 mL of the CO₂-enriched seawater was added to the ~7L batch. The batch was shaken thoroughly to mix the seawater with the CO₂-enriched seawater and the pH and temperature were measured again. Once a stable pH/temperature reading was achieved, (bottle 2) was filled. This procedure was repeated until all bottles in a treatment were filled and a CO₂ (and DIC) gradient was established across the incubation bottles. For the equilibrated and un-equilibrated NaOH treatments, I followed the same procedure but separate 0.3L and 7L batches were used for the CO₂ enrichment that had previously been amended with NaOH to elevate alkalinity from 2266.8 to $2757.4 \mu\text{mol/kg}$ prior to filling the incubation bottles. All 60 bottles were filled with 120 ± 4 g of seawater and immediately mounted on the plankton wheel (2nd of December, 2022; 17:00) under the same conditions as in Experiment 1 (i.e. 15°C, 2 rounds per minute, Fig. S1). After ~6.8 days (9th of December), bottles were removed from the plankton wheel between 9:00 and 16:00. pH and alkalinity were sampled as described in section 2.2.1.

2.2.3. Experiment 3: pH dependency of alkalinity formation from slag and olivine

Experiment 3 was designed to investigate whether a lower seawater pH would promote alkalinity formation from steel slag and olivine.

The experiment required 12 new HDPE bottles (125 mL) cleaned with double-deionised water and dried thereafter. Six of the 12 bottles were filled with 0.00644 (± 0.00007) g steel slag and the other six with 1.0003 (± 0.002) g of olivine. Three slag and three olivine bottles were filled with seawater from the same seawater source as used in Experiment 2 (Salinity= 35 ± 0.2 , alkalinity= $2263.2 \mu\text{mol/kg}$, pH_T = 7.82). pH and temperature were measured prior to filling the bottles with seawater (section 2.4.). Afterwards, the ~2L seawater batch was amended with about 80 mL of CO₂-enriched seawater as explained in section 2.2.2. This enrichment lowered the pH_T (total scale) from 7.82 to 6.85. This low pH_T (high CO₂) seawater was used to fill the other 3 slag and olivine incubation bottles. The 12 bottles with $122.8 (\pm 0.15)$ g of seawater were immediately mounted on the plankton wheel (Fig. S1) after

filling (16th of December, 2022; 16:40) under the same conditions as in Experiment 1 and 2 (i.e. 15°C, 2 rounds per minute). After ~6.8 days (23rd of December), the 12 bottles were randomly removed from the plankton wheel between 9:00 and 11:00. pH and alkalinity were sampled as described in section 2.2.1.

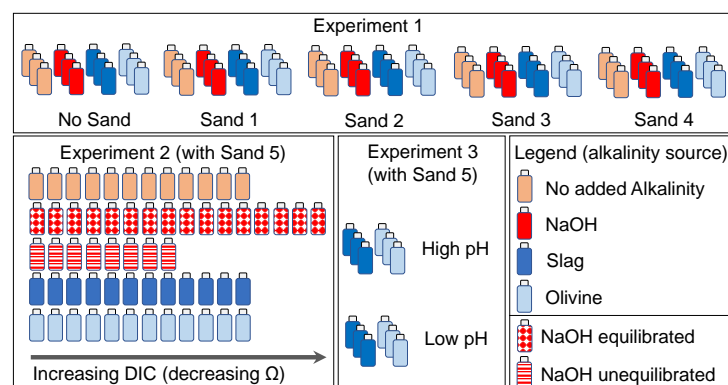


Figure 2. Design of Experiments 1, 2, and 3. Bottles represent treatments with incubation of seawater, sand, and alkalinity sources (colour code represents alkalinity source). In Experiment 2, NaOH was used as alkalinity source in two explicit scenarios as described in section 2.2.2.

2.3. Preparation and characterization of alkaline materials and beach sand

In total, 5 sand samples (0.5-1kg) were collected for Experiments 1 and 2 at Clifton Beach, Tasmania (Fig. 1, Table S2). Sampling permission was granted by the Department of Natural Resources and Environment (Authority No. ES 22314). Wet sand was sampled on the upper end of the swash zone and stored in zip bags at 15°C. Samples 1-4 were used for Experiment 1, ~24 hours after sampling while sample 5 was used for Experiment 2, ~72 hours after sampling.

Olivine rocks were sourced from the Mount Shadwell Quarry in Mortlake (Australia, Table S2). Basic oxygen slag (hereafter just called slag) was sourced from the Liberty Primary Steel – Whyalla Steelworks (Australia, Table S2). Olivine rocks and slag (Fig. S2) were crushed with a hydraulic crusher into smaller pieces of about 10 mm and then milled with a ring mill in a chrome milling pot to yield particle size distributions as shown in Fig. S3.

Wet and dry weight of the sand used for laboratory experiments was determined by weight difference of a wet and a dry sample. The wet sample (~80 g) was put into a clean plastic jar and dried for 24-72 hours at 60°C. The particle size spectra of the 5 dried sand samples as well as slag and olivine mineral were determined with a Sympatec QICPIC particle imager.

For total particulate carbon (TPC) and particulate organic carbon (POC) analyses, dried sand samples were milled for 12 minutes in a Retsch MM200 ball mill. Between 4-10 mg of each of the pulverized sand samples were weighed into 10 tin cups for TPC or 10 silver cups for POC (2 TPC and POC replicates for each sample). The POC samples were moisturized with 50µL of MilliQ water, placed for

18 hours in a dessicator that contained 36% HCl to remove all carbonates and then dried. TPC and POC samples were analysed for carbon content using a Thermo Finnigan EA 1112 Series Flash Elemental Analyser. Particulate inorganic carbon (PIC) content of the samples was then calculated as the difference between TPC and POC. Percent content of carbonates was estimated by multiplying % PIC content by the molecular weight of CaCO_3 (100 g/mol) and MgCO_3 (84.3 g/mol) for upper and lower estimates.

2.4. Carbonate chemistry, salinity, and $\text{Si}(\text{OH})_4$ measurements

pH was determined potentiometrically using a Metrohm 914 pH meter following Standard Operation Procedure 6a described in Dickson et al., (2007) but omitting the test for ideal Nernst behaviour of the electrode (ideal Nernst behaviour was assumed). A new pH electrode (Metrohm Aquatrode Plus) was calibrated on the total pH scale (pH_T) with certified reference material (CRM) TRIS buffer (batch #37), provided by Prof. Andrew Dickson's laboratory. The calibration procedure for the relevant temperature range ($\sim 8 - 18^\circ\text{C}$) followed the exact workflow as described by Ferderer et al., (2022). Precision of the pH measurement was assumed to be ± 0.015 based on experience with the probe.

Alkalinity was determined in an open cell titration following Dickson et al., (2003). Samples were measured in duplicate (each ~ 60 g) with a Metrohm 811 titration unit equipped with a Metrohm Aquatrode Plus. Alkalinity was calculated from titration curves using the Calculate function of PyCO2sys (Humphreys et al., 2020). The difference in alkalinity between duplicate titrations of the sample was on average $1.95 \mu\text{mol/kg}$ and $>75\%$ were within $4 \mu\text{mol/kg}$ ($N=185$), which was assumed to be the precision of the measurement ($\pm 2 \mu\text{mol/kg}$). Accuracy was controlled by correcting alkalinity values with CRM provided by A.G. Dickson's laboratory. Alkalinity was measured within maximally 20 days after sampling.

Salinity was measured with a Metrohm conductivity probe with a PT1000 temperature sensor connected to a Metrohm 914 conductivity meter. The probe was calibrated with DIC/alkalinity CRM from A.G. Dickson's laboratory for which a salinity of 33.464 has been reported (CRM batch 200). Conductivity was measured in mS/cm^2 and salinity was subsequently calculated on the practical salinity scale following Lewis and Perkins (1978), following the workflow described by (Moras et al., 2022). A relatively low precision of ± 0.2 was determined from repeat measurements, although precision was likely lower under field conditions where there was no temperature control.

Si concentrations for beach transects were measured 18 hours after sampling following Hansen and Koroleff, (1999). No Si measurements were conducted for Experiments 1-3.

2.5. Carbonate chemistry calculations

Carbonate chemistry conditions were calculated with the “carb function” in Seacarb (Gattuso et al., 2021), with pH_T , alkalinity, salinity, temperature, phosphate and $Si(OH)_4$ concentrations as input variables, stoichiometric equilibrium constants from (Lueker et al., 2000), and default settings for the other equilibrium constants. Si was not measured due to volume limitations, so I assumed a value of 50 $\mu\text{mol/kg}$ at the end of the experiments, when either sand, olivine, or slag were incubated. Likewise, phosphate was not measured and I assumed 2 $\mu\text{mol/kg}$ at the end of the experiments when slag was incubated. These Si and phosphate releases were based upon previous trials. Note, however, that concentrations of Si and phosphate within these ranges have negligible impact on calculated carbonate chemistry parameters (e.g. pCO_2 changes by $\sim 1 \mu\text{atm}$ when Si is assumed to be 0 instead of 50 $\mu\text{mol/kg}$).

Propagated errors in derived carbonate chemistry parameters (e.g., DIC) were calculated with the “errors” function in Seacarb using measurement precisions described in section 2.4. for pH_T (± 0.015), alkalinity ($\pm 2 \mu\text{mol/kg}$), and salinity (± 0.2), default uncertainties for equilibrium constants and temperature, and when applicable (see above) $\pm 50 \mu\text{mol/kg}$ for $Si(OH)_4$ and $\pm 2 \mu\text{mol/kg}$ for phosphate.

2.6. Calculations of the CO_2 uptake ratio (η_{CO_2}) for carbonate and non-carbonate alkalinity sources

The atmospheric CO_2 uptake ratio for OAE (η_{CO_2}) was defined as the number of moles DIC (ΔDIC) absorbed per number of moles alkalinity added ($\Delta\text{Alkalinity}$) (Tyka et al., 2022).

$$\eta_{CO_2} = \frac{\Delta\text{DIC}}{\Delta\text{Alkalinity}} \quad (5)$$

η_{CO_2} was shown to range roughly between 0.75 and 0.9 mol:mol in the surface ocean (Schulz et al., 2023; Tyka et al., 2022). However, this η_{CO_2} range only applies for alkalinity source materials that exclusively increase alkalinity without a concomitant increase in DIC when they are added to seawater ($\text{Alk}_{\text{non-carbonate}}$). Such sources comprise for example NaOH, slag, and olivine. The estimated range does not apply when all or fractions of the added alkalinity comes from carbonates ($\text{Alk}_{\text{carbonate}}$), since $CaCO_3$ contributes 2 moles of alkalinity and 1 mole of (non-atmospheric) DIC when they dissolve. In the following three paragraphs I describe how η_{CO_2} was calculated when considering varying contributions of $\text{Alk}_{\text{non-carbonate}}$ and $\text{Alk}_{\text{carbonate}}$ for a hypothetical or observed increase of $\Delta\text{Alkalinity}$. Please note that the sum of $\text{Alk}_{\text{carbonate}}$ and $\text{Alk}_{\text{non-carbonate}}$ always equals $\Delta\text{Alkalinity}$ in the following cases. Please also note that η_{CO_2} was calculated in different ways for a hypothetical case and Experiment 1 (i.e. η_{CO_2} still has the same theoretical meaning as defined in eq. 5 but was estimated in different ways).

The dependency of η_{CO_2} on the relative contribution of $\text{Alk}_{\text{carbonate}}$ and $\text{Alk}_{\text{non-carbonate}}$ was calculated as:

$$\eta_{CO_2} = \frac{DIC_{equilibrated} - \left(\frac{Alk_{carbonate}}{2}\right) - DIC_{initial}}{Alk_{non-carbonate} + Alk_{carbonate} - Alk_{initial}} \quad (6)$$

where $DIC_{initial}$ and $Alk_{initial}$ are DIC and alkalinity in seawater before alkalinity was increased, assuming a seawater pCO_2 in equilibration with the atmosphere. $DIC_{equilibrated}$ is the amount of DIC from the environment (e.g. from the atmosphere) that can be stored in seawater after the increase of $Alk_{carbonate}$ and $Alk_{non-carbonate}$, assuming seawater pCO_2 in equilibrium with the atmosphere. η_{CO_2} was first calculated for a theoretical case where $Alk_{initial}$ was 2350 $\mu\text{mol/kg}$ and $DIC_{initial}$ was calculated for the surface ocean (15°C, Salinity = 35, carbonate chemistry constants as in section 2.5), assuming a pCO_2 of 420 μatm . $Alk_{carbonate}$ and $Alk_{non-carbonate}$ were then varied in a range of scenarios (from 0 to 100% $Alk_{carbonate}$) to increase the sum of them by 1 $\mu\text{mol/kg}$. η_{CO_2} was calculated for each scenario. Next, η_{CO_2} was calculated specifically for Experiment 1 as follows: $\Delta\text{Alkalinity}$ was higher in the NaOH and slag treatments when no sand was present compared to incubations with sand (section 3.2). $\Delta\text{Alkalinity}$ was very likely $Alk_{non-carbonate}$ in all incubations while the reduced $\Delta\text{Alkalinity}$ in the incubations with sand was likely due to secondary precipitation of carbonates (section 4.2.1). Based on these conclusions, η_{CO_2} was estimated for Experiment 1 as:

$$\eta_{CO_2} = \frac{(\Delta\text{Alkalinity}_{no-sand} - \Delta\text{Alkalinity}_{sand}) \times 0.5 + \Delta\text{Alkalinity}_{sand} \times 0.86}{\Delta\text{Alkalinity}_{no-sand}} \quad (7)$$

where $\Delta\text{Alkalinity}_{no-sand}$ and $\Delta\text{Alkalinity}_{sand}$ are the changes in alkalinity measured in incubations without sand and with sand, respectively; 0.5 is the η_{CO_2} when $Alk_{non-carbonate}$ is lost via the precipitation of carbonates where 2 moles of alkalinity and 1 mol of DIC are sequestered; 0.86 is the η_{CO_2} when all $\Delta\text{Alkalinity}$ is $Alk_{non-carbonate}$ under the conditions set up in the experiments (i.e. 15°C, salinity=35; see above). Please note that $\Delta\text{Alkalinity}$ was higher in the olivine incubations when sand was present, which is opposite to the NaOH and slag incubations for reasons discussed in section 4.2.1. Therefore, η_{CO_2} was calculated assuming all $\Delta\text{Alkalinity}$ was $Alk_{non-carbonate}$ for the olivine incubations (i.e. $\eta_{CO_2} = 0.86$). For the incubations without an added alkalinity source all $\Delta\text{Alkalinity}$ was assumed to be $Alk_{carbonate}$ so that η_{CO_2} was 0.36. This assumption is justified with a 2:1 mol:mol $\Delta\text{Alkalinity}:\Delta\text{DIC}$ release ratio as observed in Experiment 2 (see next paragraph).

η_{CO_2} was also specifically calculated for Experiment 2. This required knowledge of how much of the measured $\Delta\text{Alkalinity}$ was contributed by $Alk_{carbonate}$ and $Alk_{non-carbonate}$. In the treatments where only sand was incubated, alkalinity and DIC increased roughly in a 2:1 molar ratio over the course of the experiment (i.e. $\Delta\text{Alkalinity}:\Delta\text{DIC} = 2:1$ mol:mol). Thus, it can be assumed that most of the measured alkalinity increase is $Alk_{carbonate}$. In contrast, when sand was incubated with alkaline materials, alkalinity and DIC generally increased with a molar ratio that was $>2:1$ because alkaline materials release

alkalinity without a concomitant increase of DIC. Based on these constraints, we can roughly approximate the contribution of $\text{Alk}_{\text{carbonate}}$ and $\text{Alk}_{\text{non-carbonate}}$ to the measured alkalinity increase ($\Delta\text{Alkalinity}$) as:

$$\% \text{Alk}_{\text{carbonate}} = 1 / \left(\left(\frac{\Delta\text{Alkalinity}}{\Delta\text{DIC}} \right) / 2 \right) \times 100 \quad (8)$$

Where $\% \text{Alk}_{\text{carbonate}}$ is the percentage contribution of $\text{Alk}_{\text{carbonate}}$ to $\Delta\text{Alkalinity}$. Based on eq. (8), a $\Delta\text{Alkalinity}:\Delta\text{DIC}$ of for example 8:1 mol:mol would suggest that 25% of the $\Delta\text{Alkalinity}$ is $\text{Alk}_{\text{carbonate}}$ and the other 75% $\text{Alk}_{\text{non-carbonate}}$. $\text{Alk}_{\text{carbonate}}$ and $\text{Alk}_{\text{non-carbonate}}$ were calculated with eq. 8 for all incubations in Experiment 2 and this information was then used to calculate η_{CO_2} with eq. (7). Finally, the amount of DIC that can be stored in seawater due to an increase of $\text{Alk}_{\text{carbonate}}$ and $\text{Alk}_{\text{non-carbonate}}$ (DIC_{OAE}) was calculated as:

$$\text{DIC}_{\text{OAE}} = \eta_{\text{CO}_2} * \Delta\text{Alkalinity} \quad (9)$$

for experiment 2.

2.7. Statistical analysis

Experiment 1 and 3 were analysed with a two-way analysis of variance (ANOVA) where either “sand” and “alkalinity source material” (Experiment 1) or “carbonate chemistry” and “alkalinity source material” (Experiment 3) were defined as independent variables. The dependent variables were the changes in carbonate chemistry (e.g. $\Delta\text{Alkalinity}$) over the course of the incubations. Homogeneity of variance was assessed by visually inspecting if plotted model residuals vs. fitted values were scattering similarly around 0. Normality of the residuals was assessed by inspecting qqplots where theoretical quantiles plotted against standardized residuals should ideally resemble a straight line. Such a straight-line appearance (i.e. ideal normality) was not always given, so some datasets were rank-transformed. However, transformation did not improve normality substantially so that non-transformed data was used for all analyses. Statistical differences between individual treatments were assessed with a Tukey post-hoc test. Significant differences were assumed when $p < 0.05$.

Experiment 2 was analysed by plotting $\Delta\text{Alkalinity}$ for each alkalinity source material and sand against the increase in DIC that was established via additions of CO_2 -saturated seawater (section 2.2.2). The data was fitted with the polynomial equation $a \cdot x^2 + bx + c$, where x is the amount of DIC added to each treatment and a , b , c are fit parameters. To estimate additionality of $\Delta\text{alkalinity}$ and DIC_{OAE} , the curve fitted to the sand-only data was compared to the curves fitted to the treatments.

3. Results

3.1. Beach transects

Beach transects consisted of 8-9 sampling points from just above the swash zone to 150-220 m offshore at four locations (Table S1, Fig. 1). Alkalinity showed distinct patterns across the locations. At Clifton South and Wedge, alkalinity was higher in the swash zone than in the open water. This was particularly pronounced at Clifton South with a value of 2418 $\mu\text{mol/kg}$ relative to open water values of about 2300 $\mu\text{mol/kg}$ (Fig. 3A). At Goats Beach, no such alkalinity gradient was observed across the transect, while alkalinity was lower in the swash zone at Clifton North (Fig. 3A). Wedge differed to the other locations in that alkalinity was generally lower (~ 2160 compared to ~ 2300 $\mu\text{mol/kg}$ in open water). pH_T was lowest in samples just above the swash zone at all four locations (Fig. 3B). The difference relative to open water was most pronounced at Clifton South with pH_T of 7.76 just above the swash zone compared to approximately 8.05 in the open water, while least pronounced at Goats. Gradients at Clifton North and Wedge were in between these two extremes. pH_T at Wedge was on average higher in the open water than at the other locations, i.e. 8.08 compared to 8.05 (Fig. 3B). Si(OH)_4 concentrations were highest in samples from just above the swash zone at all four locations (Fig. 3C). The most pronounced gradient was observed at Clifton South, with Si(OH)_4 of 8.6 $\mu\text{mol/L}$ just above the swash zone and ~ 1.6 $\mu\text{mol/L}$ in open water. The least pronounced gradient was observed at Goats, and intermediate gradients at Clifton North and Wedge (Fig. 3C). Overall, the data shows consistency across the three parameters measured in that Clifton South showed most pronounced trends, Goats the least pronounced trends, and Clifton North and Wedge being in between (Fig. 3).

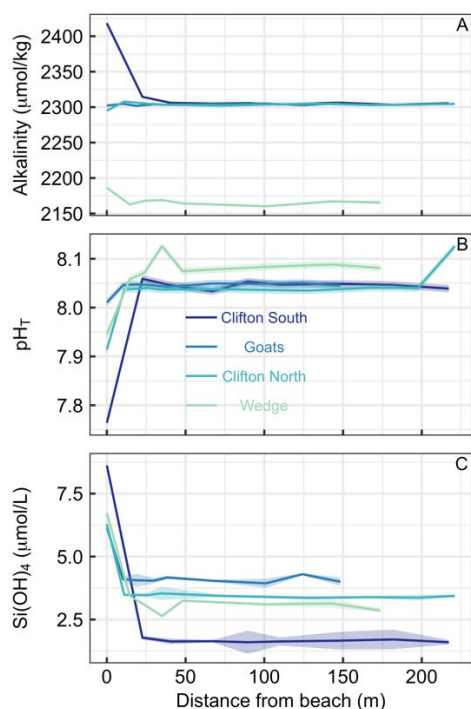


Figure 3. Transects of (A) alkalinity, (B) pH_T , and (C) Si(OH)_4 at four different beach locations in southern Tasmania (see Table S1 and Fig. 1 for locations). The first sampling was at the upper end of the swash zone and then 7-8 more samples were taken until 150-200 m offshore. Lines and shaded areas show averages and uncertainties, respectively.

3.2. Experiment 1

Alkalinity increased over the course of the 6.8 days in all treatments where alkaline materials were added (Fig. 4). Changes in alkalinity ($\Delta\text{Alkalinity}$) were between ~ 610 - $400 \mu\text{mol/kg}$ for the slag, ~ 420 - $290 \mu\text{mol/kg}$ for the NaOH, and 280 - $370 \mu\text{mol/kg}$ for the olivine treatment. In contrast, $\Delta\text{Alkalinity}$ changed very little (i.e. $\Delta\text{Alkalinity} \leq 6 \mu\text{mol/kg}$) when no alkaline materials were added. (Please note that an important outlier was observed in Sand 2 where $\Delta\text{Alkalinity}$ was $87.3 \mu\text{mol/kg}$ which will be discussed in section 4.2.2.). The two-way ANOVA revealed significant effects of (1) the type of sand, (2) the type of alkalinity source, and (3) the interaction of these two on $\Delta\text{Alkalinity}$ ($p < 0.05$). For the slag and the NaOH treatment, $\Delta\text{Alkalinity}$ was significantly higher when these were incubated without sand but only small differences were observed across the four sand samples. In contrast, $\Delta\text{Alkalinity}$ was slightly lower in the olivine treatment when no sand was present during incubations although the difference was only significant relative to olivine incubated in Sand 4 (Fig. 4A).

Changes in pH_T (ΔpH_T) reflected the patterns described for $\Delta\text{Alkalinity}$ (Fig. 4B). ΔpH_T was highest in the slag and the NaOH treatment when no sand was added, while this difference between the presence and absence of sand was not observed for olivine. ΔpH_T was slightly negative in treatments where no

alkalinity source was added to the incubated sand samples. The two-way ANOVA revealed significant effects of sand, alkalinity source and their interaction on ΔpH_T ($p < 0.05$).

η_{CO_2} was prescribed to be 0.36 when sand without an anthropogenic alkalinity source was incubated and 0.86 for olivine incubations (see section 2.6). Calculated η_{CO_2} for NaOH and slag treatments were slightly lower due to relatively lower $\Delta\text{Alkalinity}$ in the presence of sand than without the presence of sand (Fig 4C). Statistics are not provided for η_{CO_2} data because assumptions of the ANOVA model were heavily violated.

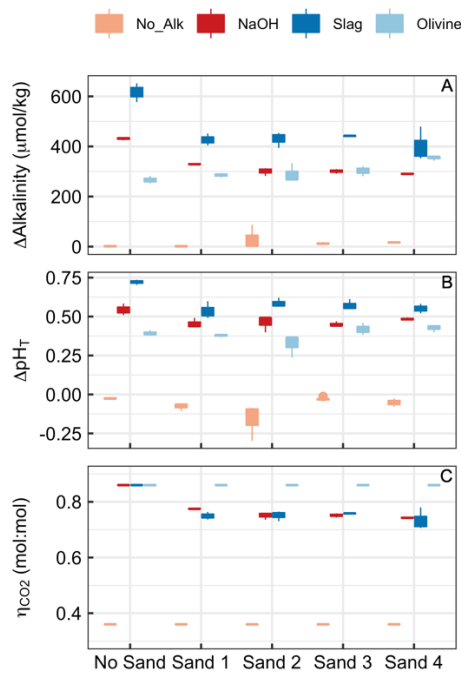


Figure 4. Results of Experiment 1. Changes of (A) alkalinity and (B) pH_T from the beginning to the end of the 6.8 days experiment. (C) η_{CO_2} at the end of the experiment. Boxplots are based on three replicates per treatment. Colours refer to the added alkalinity source (No_Alk means no alkalinity source was added). The alignment on the x-Axis indicates if or which sand sample was present in the incubation bottles (“No Sand” means no Sand was added).

3.3. Experiment 2

The additions of CO_2 -enriched seawater established a gradient of increasing DIC and accordingly a decline in pH_T and Ω_{Arg} (Table S3). The rationale for this setup was that beach sediments can contain high amounts of respiratory CO_2 so that anthropogenic alkalinity added to beaches has a high likelihood to be exposed to such high CO_2 conditions (Liu et al., 2021; Perkins et al., 2022; Reckhardt et al., 2015)(Liu et al., 2021; Perkins et al., 2022; Reckhardt et al., 2015). Fig. 5 shows $\Delta\text{Alkalinity}$ along the DIC gradient for different alkalinity source materials (NaOH, slag, olivine) and compares this to

Δ Alkalinity along the same DIC gradient where only sand from a beach was present. The “sand only” data is identical in all four plots (orange lines in Fig. 5). It shows that Δ Alkalinity is close to zero in the sand-only incubations when no DIC is added but increases exponentially with increasing DIC additions up to 537 $\mu\text{mol/kg}$.

OAE via NaOH additions was set up in two different scenarios (Fig. 5A, B). In the first scenario, the carbonate system was equilibrated with atmospheric CO_2 after the NaOH deployment and before exposed to the sand (Fig. 5A). Such a scenario could occur when NaOH is added to the ocean, but subsequent air-sea CO_2 influx fully equilibrated the NaOH-induced seawater CO_2 deficit before any interactions with sediments occur. Likewise, equilibration of CO_2 -deficient seawater could be established within the electrochemical OAE facility and thus before the alkalinity-enhanced seawater is discharged back into the ocean. The equilibrated setup leads to a gradient in Ω_{Arg} from 2.1 to 0.2 at the beginning of the 6.8 days incubations (highest Ω_{Arg} at the lowest DIC addition). In the second scenario, the carbonate system was not equilibrated, thereby assuming that a NaOH-enriched patch of seawater would be exposed to sand sediments before it had taken up atmospheric CO_2 (Fig. 5B). Here, initial Ω_{Arg} ranges from 7.1 to 2.3 along the DIC gradient. In the equilibrated scenario, Δ Alkalinity was 482 $\mu\text{mol/kg}$ when no DIC was added and increased exponentially to 973 $\mu\text{mol/kg}$ at the highest DIC addition (Fig. 5A). In the unequilibrated scenario, Δ Alkalinity was 344 $\mu\text{mol/kg}$ when no DIC was added and increased to 474 $\mu\text{mol/kg}$ at the highest DIC addition. However, in contrast to the equilibrated treatment, the Δ Alkalinity increase in the unequilibrated treatment weakened along the DIC gradient and Δ Alkalinity was lower than in the sand-only treatment when the DIC addition was >400 $\mu\text{mol/kg}$ (Fig. 5B).

In the slag treatment, Δ Alkalinity was 521 $\mu\text{mol/kg}$ when no DIC was added. Δ Alkalinity increased exponentially along the DIC gradient to 814 $\mu\text{mol/kg}$. The increase of Δ Alkalinity was less pronounced than in the sand-only treatment. Overall, the slag data showed more scatter relative to the other alkalinity source materials and sand-only treatments (Fig. 5C).

In the olivine treatment, Δ Alkalinity was 258 $\mu\text{mol/kg}$ when no DIC was added. Δ Alkalinity increased exponentially with increasing DIC additions to 453 $\mu\text{mol/kg}$ although much less pronounced than in the sand-only treatment. Δ Alkalinity was lower in the olivine than in the sand-only treatment when DIC additions were >350 $\mu\text{mol/kg}$ (Fig. 5C).

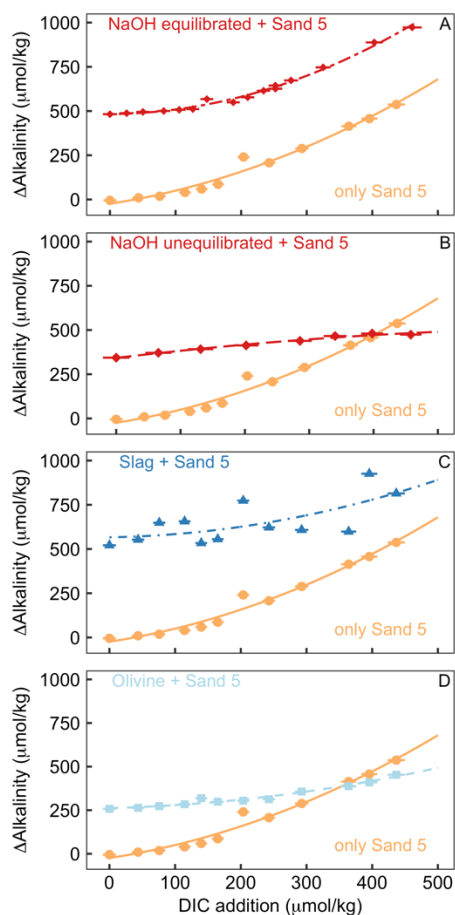


Figure 5. Results of Experiment 2. All panels show the change in alkalinity from the beginning to the end of the 6.8 days experiment along a gradient of DIC added to the incubation bottles (DIC values shown here refer to the values calculated from alkalinity and pH at the start of the experiment). The orange data displayed on all panels show Δ Alkalinity for incubations where only sand was incubated. The other data on each panel show Δ Alkalinity when sand was incubated with an external alkalinity source or addition scenario. Corresponding Ω_{Arg} and pH_T values for all scenarios are provided in Table S3. (A) Sand and NaOH equilibrated with atmospheric CO_2 upon addition; (B) Sand and NaOH which was not equilibrated with atmospheric CO_2 upon addition; (C) Sand and slag; (D) Sand and olivine.

3.4. Experiment 3

Experiment 3 tested if there is a carbonate chemistry dependency of alkalinity release by olivine and slag (Fig. 6). The two-way ANOVA revealed a significant influence of pH_T on the release of alkalinity from olivine and slag (Fig. 6, please note that pH_T was used for analysing the data but other carbonate chemistry parameters could also be the driver of the response). Slag released 707 ± 61 $\mu\text{mol/kg}$ alkalinity when incubated within a pH_T from initially 7.82 to 8.67 at the end of the 6.8 days incubation. Within the lower pH_T range from 6.86-8.39, slag released 805 ± 86 $\mu\text{mol/kg}$. Olivine released 234 ± 36 $\mu\text{mol/kg}$

when incubated within a pH_T from initially 7.82 to 8.20 at the end of the 6.8 days incubation. Within the lower low pH_T range from 6.86-7.63, olivine released $298 \pm 8 \mu\text{mol/kg}$ (Fig. 5).

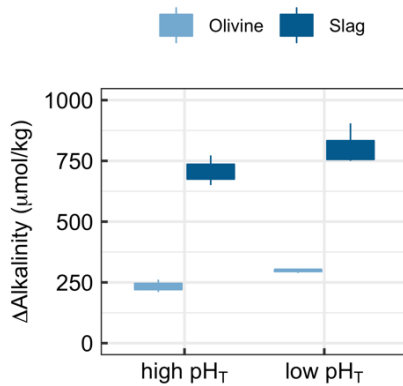


Figure 6. Results of Experiment 3. Changes in alkalinity from the beginning to the end of the 6.8 days experiment when olivine or slag were incubated (without sand) under high (initially 7.82) or low pH_T (initially 6.85). $\Delta\text{Alkalinity}$ was significantly higher under low pH_T ($p < 0.05$).

4. Discussion

4.1. Carbonate-derived alkalinity is less efficient for CDR than non-carbonate-derived alkalinity

Section 2.6. introduced equations which show that alkalinity originating from carbonates ($\text{Alk}_{\text{carbonate}}$) has considerably less capacity to absorb CO_2 than alkalinity originating from non-carbonate sources such as olivine, slag, or NaOH ($\text{Alk}_{\text{non-carbonate}}$). The large influence of this chemical constraint on OAE is exemplified in Fig. 7. Here, the uptake potential for atmospheric CO_2 per mol alkalinity added to the ocean (η_{CO_2}) is shown as a function of the carbonate contribution to the alkalinity source. When all $\Delta\text{Alkalinity}$ delivered via OAE originates from non-carbonate sources (e.g., NaOH, slag, olivine), then η_{CO_2} equals 0.86. η_{CO_2} declines linearly with an increasing contribution $\text{Alk}_{\text{carbonate}}$ to $\Delta\text{Alkalinity}$ to the lowest theoretical value for η_{CO_2} of 0.36, which is reached when OAE provides all alkalinity as $\text{Alk}_{\text{carbonate}}$ (Fig. 7).

The dependency of η_{CO_2} on the alkalinity source material (Fig. 7) has important implications for OAE methods that aim to utilise CaCO_3 as alkalinity source (Renforth et al., 2022; Wallmann et al., 2022; Harvey, 2008; Rau and Caldeira, 1999). The molar efficiency for atmospheric CO_2 sequestration of OAE is $>50\%$ lower when using carbonates (e.g. CaCO_3). Or put differently, OAE approaches utilising CaCO_3 as alkalinity source would have to increase alkalinity by more than twice as much to generate similar CDR compared to methods that use non-carbonates (e.g. NaOH, slag, or olivine). Importantly, while this disadvantage of carbonate sources of alkalinity appears to be substantial, it is not the only

important factor determining the potential of such OAE approaches. It is possible that the use of carbonates still holds higher potential, for example because limestone is relatively abundant (Caserini et al., 2022), can dissolve quickly (Renforth et al., 2022), or because it contains fewer components potentially affecting marine organisms (Bach et al., 2019). Nevertheless, the dependency of η_{CO_2} on the alkalinity source (Fig. 7) needs to be considered when assessing the efficiency of different OAE methods, as will become apparent in section 4.2.

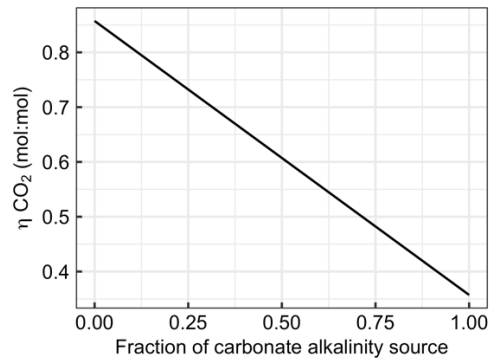


Figure 7. Changes in η_{CO_2} with the fraction alkalinity originating from carbonates (e.g. CaCO_3 dissolution). The x-axis ranges from 0 (all alkalinity originates from non-carbonate sources such as NaOH, slag, or olivine) to 1 (all alkalinity originates from carbonate sources such as CaCO_3 or MgCO_3).

4.2. The additionality problem of OAE

The experiments considered here investigate coastal applications of OAE, for example when ground materials or NaOH are exposed to beaches or sandy sediments. In the experiments, the treatments where only sand was incubated constitute the baseline system while incubations of sand and an alkalinity source constitute the OAE deployments. Both the baseline system and the OAE deployment were run in parallel under identical conditions. To assess the additionality of OAE, CO_2 sequestration achieved through an OAE deployment must be compared to the baseline state where no such deployment occurred (see eq. 4). As such, additionality can be affected through processes that affect the OAE deployment directly (section 4.2.1.), or when the OAE deployment alters the baseline state of the system (section 4.2.2.).

4.2.1. Change of additionality through interaction of alkalinity sources with sand

The $\Delta\text{Alkalinities}$ determined in Experiment 1 were lower in NaOH and slag incubations with sand than in incubations without sand. The reduction in the presence of sand was likely due secondary precipitation of carbonates, which is promoted when Ω_{CaCO_3} is elevated and/or there are particles (here

sand), which provide nucleation sites for CaCO_3 precipitation (Moras et al., 2022; Fuhr et al., 2022; Zhong and Mucci, 1989).

In contrast to the NaOH and slag incubations, the olivine incubations generated more $\Delta\text{Alkalinity}$ when sand was present, even though the enhancement was small and only in one case statistically significant (i.e. No Sand vs Sand 4; Fig. 4A). This contrasting observation can be explained as follows. First, $\Delta\text{Alkalinity}$ was generally lower in the olivine incubations than in the NaOH and slag incubations when no sand was present ($266 \pm 14.8 \mu\text{mol/kg}$ for olivine vs. $>420 \mu\text{mol/kg}$ for NaOH and slag). Moras et al., (2022) have shown that the onset of secondary precipitation depends on $\Delta\text{Alkalinity}$ and they observed no secondary precipitation over a 40 day experimental incubation when $\Delta\text{Alkalinity}$ was $\sim 250 \mu\text{mol/kg}$ ($\Omega_{\text{Arg}} \sim 4$). This suggests that the $266 \pm 14.8 \mu\text{mol/kg}$ $\Delta\text{Alkalinity}$ generated by olivine did not elevate Ω_{Arg} to high enough levels to induce noticeable secondary precipitation within 6.8 days. However, the absence of such secondary precipitation cannot explain why $\Delta\text{Alkalinity}$ increased in the presence of sand. It is possible that the sand itself released alkalinity via carbonate dissolution as a very small increase in $\Delta\text{Alkalinity}$ was also observed in some sand-only incubations (e.g. $17.4 \pm 2.6 \mu\text{mol/kg}$ in Sand 4; Fig. 4A). However, Ω_{Arg} was higher in the olivine incubations as in the sand-only treatment so that a release of carbonate alkalinity seems unlikely. It is also unlikely that the pH differences between olivine-only and olivine+sand incubations drove this trend. While Experiment 3 underscores that lower pH promotes the release of alkalinity from olivine (Fig. 6), pH_T was higher in the olivine+sand treatment where significantly more alkalinity was released (see Sand 4 in Fig. 5A). What appears as a plausible explanation is that the sand caused physical destruction of coatings that develop on the olivine particles during dissolution and are known to reduce dissolution rates (Oelkers et al., 2018). Indeed, the dissolution-enhancing role physical abrasion has been hypothesised to increase OAE efficiency when using olivine (Schuiling and de Boer, 2010), as has recently been confirmed by (Flipkens et al., 2023).

η_{CO_2} is reduced when the presence of sand catalyses secondary precipitation (Fig. 5C). Consequently, the amount of DIC that can be sequestered via OAE declines. Among other factors, the degree of alkalinity loss due to secondary precipitation depends on the duration carbonate supersaturated water is exposed to the sand. The experiments presented here lasted for 6.8 days and it is likely that secondary precipitation would have proceeded (and η_{CO_2} further declined) if the experiments had lasted for longer. Indeed, Moras et al., (2022) observed that secondary precipitation catalysed by particles only slowed down once Ω_{Arg} reached ~ 2 . In the experiments presented here, Ω_{Arg} was generally >5 at the end of the study. A back-of-the-envelope carbonate chemistry calculation with seacarb suggests that a decline until Ω_{Arg} reaches 2 via carbonate precipitation (i.e. alkalinity and DIC decline in a 2:1 molar ratio) would have reduced alkalinity by $\sim 560 \mu\text{mol/kg}$ for the NaOH and $840 \mu\text{mol/kg}$ for the slag incubations, respectively. In both cases the alkalinity after the OAE perturbation would be lower than before but

atmospheric CO₂ uptake would still occur ($\eta_{\text{CO}_2} = 0.39$ for NaOH and 0.37 for slag) because the pCO₂ is still slightly lower than before the perturbation (Moras et al., 2022).

4.2.2. Reduction of additionality through modification of baseline alkalinity formation

One interesting observation was made during a sand-only incubation of Experiment 1 (i.e. “No_Alk in Fig. 4). For Sand 2, $\Delta\text{Alkalinity}$ was about 85 $\mu\text{mol/kg}$ higher in one replicate bottle than in the other two. This difference was due to a small arthropod (likely a sand flea) that was unintentionally added to the incubation bottle where the high $\Delta\text{Alkalinity}$ was observed. The arthropod was still alive at the end of the 6.8 incubation period. During those 6.8 days, the organism respired, thereby reducing Ω_{Arg} , and causing alkalinity release from the sand via CaCO₃ dissolution. This observation pointed out that the baseline system can already release substantial amounts of alkalinity even before OAE is implemented given sufficient respiration. Indeed, the in-situ observations at Clifton South suggest that alkalinity release occurs in the baseline system used here (section 3.1). Furthermore, there is widespread evidence from the literature that beaches release alkalinity via CaCO₃ dissolution (Liu et al., 2021; Perkins et al., 2022; Reckhardt et al., 2015). These insights collectively inspired Experiment 2, where a DIC gradient (high to low Ω_{Arg}) was set up to test if natural alkalinity release via CaCO₃ dissolution would be influenced by anthropogenic alkalinity release via OAE.

Experiment 2 demonstrated that the release of natural alkalinity can be disturbed by the addition of anthropogenic alkalinity sources (Fig. 8). Fig. 8A illustrates the additionality of alkalinity release, calculated by subtracting $\Delta\text{Alkalinity}$ from sand-only incubations (represented by the orange lines in Fig. 5 panels A-D) from $\Delta\text{Alkalinity}$ in sand+alkalinity incubations (represented by the red and blue lines). Fig. 8A reveals that the additionality of $\Delta\text{Alkalinity}$ declines with increasing amounts of added DIC. The reason for this trend is that the alkalinity sources added to the incubation bottles buffered the DIC-induced pH decline. This buffering elevated Ω_{Arg} during the incubations, resulting in a reduced release of natural alkalinity through CaCO₃ dissolution. Or in simpler terms, by adding a new buffer system via OAE (NaOH, slag, or olivine), a natural buffer system (CaCO₃ dissolution) is partially replaced. In cases where olivine or non-equilibrated NaOH was tested, the additionality of $\Delta\text{Alkalinity}$ became even negative when DIC additions were >350 and >400 $\mu\text{mol/kg}$, respectively (Fig. 8A).

Alkalinity release is generally seen as a good indicator for the amount of CO₂ that can be removed per mole alkalinity enhancement (η_{CO_2}). However, as discussed in section 4.1., η_{CO_2} also critically depends on whether the released alkalinity is $\text{Alk}_{\text{carbonate}}$ or $\text{Alk}_{\text{non-carbonate}}$. In Experiment 2, η_{CO_2} varies greatly depending on the alkalinity source and the amount of DIC added to the incubation (Fig. 8B). η_{CO_2} is low for sand-only incubations because basically all $\Delta\text{Alkalinity}$ is $\text{Alk}_{\text{carbonate}}$, whereas it is substantially higher in treatments with an anthropogenic $\text{Alk}_{\text{non-carbonate}}$ source. For olivine, η_{CO_2} was around 0.7 up

until the highest DIC additions where η_{CO_2} declines slightly. This is lower than for slag, where η_{CO_2} remains close to the theoretical maximum of 0.86. The difference between slag and olivine could be due to faster dissolution of slag, which elevates Ω_{Arg} before substantial CaCO_3 dissolution had occurred. In contrast, olivine dissolves more slowly (Fuhr et al., 2022; Montserrat et al., 2017; Hangx and Spiers, 2009), so that some CaCO_3 dissolution may have occurred before olivine dissolution elevated Ω_{Arg} enough to limit further CaCO_3 dissolution. (Please note, however, that this explanation does not explain why η_{CO_2} is also lower than in slag incubations at low DIC additions, where Ω_{Arg} was high enough to limit CaCO_3 dissolution from the start). The reason for the decreasing η_{CO_2} in the equilibrated NaOH scenario (Fig. 8B) is an increasing contribution of $\text{Alk}_{\text{carbonate}}$ to $\Delta\text{Alkalinity}$. It is important to note that for the same added DIC, Ω_{Arg} is much lower in the equilibrated NaOH scenario than in unequilibrated NaOH scenario (e.g. 0.28 vs. 2.9 at $\sim 400 \mu\text{mol/kg}$ added DIC for the equilibrated and unequilibrated NaOH scenarios, respectively). This lower Ω_{Arg} is because the equilibrated scenario simulates that atmospheric CO_2 has already been absorbed by the alkalinity-enhanced seawater. Accordingly, alkalinity-enhanced seawater that has been equilibrated with atmospheric CO_2 interacts with beach sediments at a lower Ω_{Arg} than if the alkalinity-enhanced seawater was unequilibrated. As such, the equilibrated OAE scenario causes less reduction of natural alkalinity release from sediments via CaCO_3 dissolution.

Measurements and estimates of $\Delta\text{Alkalinity}$ and η_{CO_2} enabled calculation of how much DIC could be maximally stored by the generated alkalinity (i.e., DIC_{OAE} as calculated in eq. 9 is shown in Fig. 8C). DIC_{OAE} increases with higher DIC additions due to the release of alkalinity via CaCO_3 dissolution. However, the increase is less pronounced as observed for $\Delta\text{Alkalinity}$ (Fig. 8A) because $\text{Alk}_{\text{carbonate}}$ from CaCO_3 dissolution is less efficient in sequestering environmental CO_2 than $\text{Alk}_{\text{non-carbonate}}$ from NaOH, slag, or olivine (section 4.1).

To calculate the additionality of DIC_{OAE} , I subtracted DIC_{OAE} of the sand-only incubations (baseline) of DIC_{OAE} of the OAE scenarios (Fig. 8D). The additionality of DIC_{OAE} is arguably the most important parameter to assess whether an OAE deployment has led to the net sequestration of CO_2 . In the case of the equilibrated NaOH and slag scenarios, the additionality of DIC_{OAE} was constant over the applied gradient, suggesting that the release of $\text{Alk}_{\text{carbonate}}$ via CaCO_3 dissolution led to similar DIC_{OAE} potential in the sand-only scenario and these two OAE scenarios. In contrast, the additionality of DIC_{OAE} declined in the olivine scenario because there was relatively more $\text{Alk}_{\text{carbonate}}$ release in the sand only scenario than in the olivine scenario (Fig. 8D). Importantly, however, the additionality of DIC_{OAE} remains positive up until the highest DIC addition, which is in stark contrast to the additionality of $\Delta\text{Alkalinity}$ (compare Fig 8A and D). This means that the addition of olivine maintained a positive CO_2 sequestration potential even though less alkalinity was generated in the olivine treatment than in the sand-only treatment (Fig. 8C). The reason for this counterintuitive observation is simply that the $\text{Alk}_{\text{non-}}$

carbonate released by olivine has more potential to sequester CO₂ than the Alk_{carbonate} released via CaCO₃ dissolution.

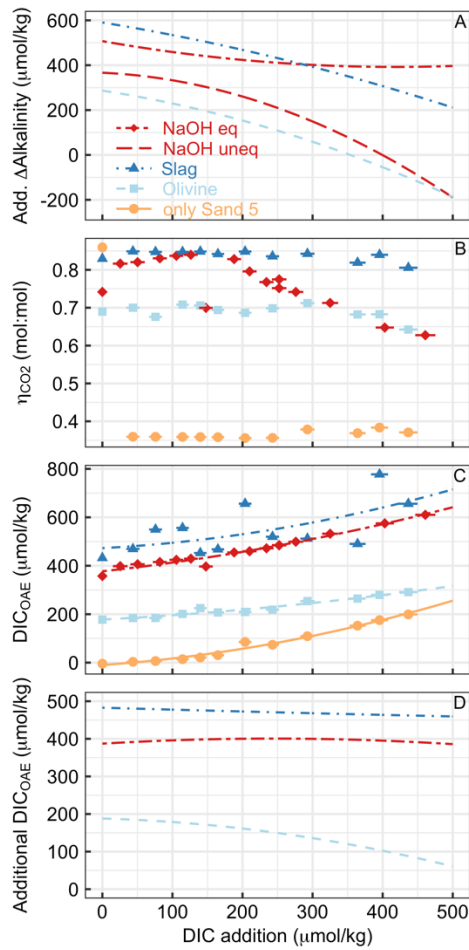


Figure 8. Various measures of OAE efficiency under increasing additions of DIC in Experiment 2 (DIC could for example be CO₂ from the respiration of organic material in sediments). (A) The additionality of ΔAlkalinity. (B) η_{CO2} at the end of the experiment. Please note that the extreme outlier at lowest DIC addition in the sand-only treatment was likely due to measurement uncertainty. (C) DIC_{OAE}, i.e., how much seawater CO₂ could have potentially been absorbed with the amount of ΔAlkalinity provided by the various alkalinity sources. (D) The additionality of DIC_{OAE}. Please note that panels (B-D) only show data for the equilibrated NaOH scenario. I omitted the unequilibrated scenario for logical reasons, i.e., because the core assumption in this scenario (no CO₂ equilibration with the atmosphere after OAE) is at odds with the necessary assumption of CO₂ equilibration to calculate η_{CO2} (section 2.6).

4.3. Relevance of the additionality problem

Modifications of additionality can occur when OAE triggers subsequent alkalinity loss through biotic and abiotic carbonate precipitation (section 4.2.1.). This feedback has been widely discussed and is

already a predominant topic in OAE research (Hartmann et al., 2013; Bach et al., 2019; Moras et al., 2022; Fuhr et al., 2022; Hartmann et al., 2023). Not yet discussed is the modification of additionality that may occur when anthropogenic alkalinity sources (via OAE) modify the release of natural alkalinity (section 4.2.2.). Thus, I will focus on the relevance of this second pathway of additionality modification in the following paragraphs.

The experiments conducted here tested how anthropogenic alkalinity sources can interact with beach sand in a setting that assumes constant mixing, inspired by conditions observed in a high energy wave impact zone. This setting was chosen based on the widely discussed OAE implementation strategy of adding olivine powder to beaches. The results suggest that the “additionality problem” needs to be considered for this specific OAE approach. However, the wave impact zone comprises a tiny fraction of the coastal ocean and the question is to what extent the additionality problem also applies to the vast shelf, bank, embayment and reef areas where OAE could also be implemented (Feng et al., 2017; Meysman and Montserrat, 2017; Mongin et al., 2021).

The coastal ocean is a net sink of ~ 36 Tmol/year alkalinity via CaCO_3 burial (Middelburg et al., 2020), but considerable amounts of alkalinity are also generated in the various coastal sediments via CaCO_3 dissolution (one estimate suggests ~13 Tmol/year; (Krumins et al., 2013)). The dissolution depends on the solubility of CaCO_3 present in the sediments and pore water Ω_{CaCO_3} (Middelburg et al., 2020). Conditions for dissolution are generally favourable in coastal ocean sediments because soluble forms of CaCO_3 occur more frequently and relatively high supply of organic matter lowers Ω_{CaCO_3} (Krumins et al., 2013; Lunstrum and Berelson, 2022; Morse et al., 1985). Thus, the introduction of an anthropogenic buffer via OAE (which increases Ω_{CaCO_3}) is likely to cause a reduction of alkalinity release from the seafloor.

Indeed, more soluble forms of CaCO_3 were shown to protect less soluble forms of CaCO_3 from dissolution at the seafloor (Sulpis et al., 2022). Furthermore, an experiment exposed a coral reef to moderate levels of increased alkalinity ($\Delta\text{Alkalinity} = \sim 50 \mu\text{mol/kg}$) and found a net increase of reef calcification, with some evidence suggesting that the measured effect was due to reduced reef dissolution (Albright et al., 2016). Anthropogenic alkalinity sources (e.g. NaOH, slag, olivine) introduced via OAE can be considered to have a similar effect and reduce natural alkalinity release via CaCO_3 dissolution. It is worth noting that the negative effect of anthropogenic alkalinity on natural alkalinity release may also occur in the open surface ocean. Here, part of the alkalinity bound in particulate form via biotic calcification re-dissolves, for example in corrosive microenvironments such as zooplankton or marine snow (Subhas et al., 2022; Milliman et al., 1999; Sulpis et al., 2021). If anthropogenic alkalinity introduced via OAE reduces this natural dissolution of CaCO_3 in the surface ocean, then less alkalinity would remain in the surface ocean and the additionality of OAE would be reduced (Bach et al., 2019). Thus, the “additionality problem” of OAE could be widespread and not restricted to the specific environment studied experimentally in this paper.

Another interesting aspect to consider is the time and scale-dependency of the additionality problem. A detectable slow-down of natural alkalinity formation may occur in the environment where anthropogenic alkalinity was added (as observed in the experiments presented here). Such an “acute” additionality problem may be comparatively easy to associate with the responsible OAE deployment and there may be straight-forward ways to mitigate it. (see section 4.4 and Box 1). However, the problem could turn from “acute” to “chronic” over much longer timescales should OAE be up-scaled to climate-relevance and cause a significant increase of Ω throughout the ocean. In the chronic scenario, anthropogenic alkalinity may partially replace the “natural” alkalinity release enforced by fossil fuel CO₂ neutralization via carbonate dissolution (Archer et al., 1998). A chronic additionality problem would unlikely be attributable to individual OAE deployments and suggested mitigation measures described in section 4.4. and Box 1 would not work. Indeed, similar chronic problems for CDR imposed by Earth system feedbacks have already been described, for example the possible weakening of natural terrestrial and marine CO₂ sinks due to CDR implementation (Keller et al., 2018). However, assessing whether the hypothesis of a chronic additionality problem is valid remains to be seen and will require more targeted follow-up research.

4.4. Possible ways to manage the additionality problem

This section discusses potential pathways to manage an acute additionality problem. The discussion is accompanied with Box 1, which translates thoughts raised here into suggestions how practitioners (e.g. OAE start-ups) could deal with acute additionality problems.

To manage the additionality problem, it is important to monitor the natural alkalinity release in a designated OAE deployment site before OAE is implemented. Natural alkalinity release occurs in all coastal habitats (Krumins et al., 2013; Aller, 1982; Perkins et al., 2022; Liu et al., 2021) and recent evidence suggests that even small CaCO₃ content in sediments is sufficient to yield high alkalinity release rates (Lunstrum and Berelson, 2022). As such, dissolution is not restricted to CaCO₃ rich sediments and avoiding these may therefore not mitigate the additionality problem. More crucial than the CaCO₃ content appears to be the supply of organic matter to the seafloor, which provides respiratory CO₂ needed for CaCO₃ dissolution and associated alkalinity release (but note that organic matter supply also drives organic or other inorganic alkalinity release (Krumins et al., 2013; Aller, 1982; Lunstrum and Berelson, 2022; Perkins et al., 2022; Liu et al., 2021). Therefore, it may be useful to avoid OAE near sediments exposed to high organic matter load to reduce the interference of anthropogenic alkalinity with natural alkalinity release.

Another mitigation pathway for the additionality problem is dilution. When anthropogenic alkalinity is diluted quickly then there is less chance for the new buffer system to generate oversaturated Ω in seawater, sediment pore waters, or other microenvironments. Indeed, the data from the beach transects show that alkalinity (and Si(OH)₄) deviations in the upper end of the swash zone were quickly lost upon

moving offshore (Fig. 3). The experiments presented here do not allow for such dilution as they are performed in enclosed volumes. They can therefore be considered a more extreme case, which do not correctly represent the vastness of the ocean and its volume. Indeed, previous experiments investigating the risk of alkalinity loss after OAE due to secondary precipitation found that dilution effectively mitigates the secondary precipitation problem (Moras et al., 2022). It is very likely that dilution is similarly effective to mitigate the additionality problem.

Finally, the data presented here clearly show that the additionality problem scales with the degree of CaCO_3 oversaturation introduced through the anthropogenic alkalinity source. This is most obvious when comparing the equilibrated with the unequilibrated NaOH OAE scenario. The increase of Ω_{CaCO_3} is much more pronounced in the unequilibrated scenario because atmospheric CO_2 has not yet entered the seawater and brought down Ω_{CaCO_3} to levels it was before the OAE perturbation. As such, the additionality problem will be much more pronounced when an alkalinity source interacts with naturally alkalinity releasing sediments before the OAE-perturbed seawater has been equilibrated with atmospheric CO_2 . Nevertheless, a close look at Fig. 4A (equilibrated NaOH) shows that even the relatively small increase of Ω_{CaCO_3} that coincides with OAE fully equilibrated with atmospheric CO_2 , can reduce natural alkalinity release. Thus, atmospheric CO_2 equilibration following OAE mitigates the additionality problem but cannot fully avoid it.

Box 1. Suggestions for OAE practitioners.

Research much beyond the present study is needed to better constrain the magnitude of the additionality problem and evaluate its relevance for OAE. However, real-world OAE assessments and ambitions for implementation are already underway so that some initial guidance on the additionality problem may be important already now, even if based on limited evidence. This Box translates thoughts discussed in section 4 into suggestions directed to those working on the implementation of OAE. Importantly, practitioners should remain critical about these suggestions (they may change with further knowledge gain) and apply at own risk.

- With the currently limited understanding of the additionality problem, it may be best to avoid it as much as possible.
- Choose a field site with high dilution. Interaction of anthropogenic alkalinity with the natural alkalinity cycle are less likely to occur when alkalinity-enhanced seawater is quickly mixed with unperturbed seawater. As such, volumes with restricted exchange (e.g. bays, lagoons, fjords) may be more problematic.
- Enable fast equilibration of the alkalinity-enhanced seawater with atmospheric CO_2 . The influx of atmospheric CO_2 returns Ω_{CaCO_3} of alkalinity-enhanced seawater to values closer to unperturbed seawater and thus has less potential to affect CaCO_3 dissolution or precipitation.

- When possible, restrict contact of anthropogenic alkalinity with sediments to reduce interactions at hotspots of natural alkalinity cycling. This suggestion is not feasible for OAE implementation via coastal enhanced weathering where alkaline minerals are added to sediments (Eisaman et al., 2023). For this OAE strategy, it is suggested to prefer sediments depleted in organic matter where less “fuel” is available for respiration and associated carbonate dissolution (i.e. natural alkalinity release).
- Frameworks to monitor, report, and verify the success of OAE should include sediment interactions and account for the additionality problem.

5. Conclusion and outlook

The additionality problem described herein could influence the effectiveness of OAE. It suggests that interference of anthropogenic alkalinity with the natural alkalinity cycle must be assessed as a factor that can modify the OAE efficiency. The arguments provided in the discussion suggest that the additionality problem is potentially widespread, even though the dataset presented here only considers OAE near or on wave-exposed beaches. Future research should aim to confirm or dismiss these arguments and to better understand the extent of the problem.

The additionality problem adds a layer of complexity to monitoring, reporting, and verification of CO₂ removal with OAE. Strictly speaking, it is not sufficient to monitor the generation (e.g., via NaOH, slag, or olivine dissolution) and potential loss (e.g., via biotic and abiotic precipitation) of anthropogenic alkalinity after its generation. It also needs to be assessed to what extent anthropogenic alkalinity alters the baseline removal or delivery of natural alkalinity. It will be crucial to understand whether the anthropogenic acceleration of the alkalinity cycle in the oceans via OAE could slow down the natural alkalinity cycle.

Competing interests

The author declares no competing interests.

Acknowledgements

I thank Jiaying Guo and Bec Lenc for providing particle size spectra, the Moyne Shire Council for providing olivine samples, Bradley Mansell from Liberty Primary Steel for providing steel slag aggregates, and the Central Science Laboratory at the University of Tasmania for particulate carbon analyses. This research was funded through a Future Fellowship Award by the Australian Research Council (FT200100846) and by the Carbon-to-Sea Initiative, a non-profit dedicated to evaluating Ocean Alkalinity Enhancement.

Data availability statement

All data and evaluation scripts (for R) generated herein are available for download at zenodo.org under the doi:10.5281/zenodo.8191516.

References

- Adkins, J. F., Naviaux, J. D., Subhas, A. V, Dong, S., and Berelson, W. M.: The Dissolution Rate of CaCO_3 in the Ocean, <https://doi.org/10.1146/annurev-marine-041720>, 2020.
- Albright, R., Caldeira, L., Hosfelt, J., Kwiatkowski, L., Maclaren, J. K., Mason, B. M., Nebuchina, Y., Ninokawa, A., Pongratz, J., Rieke, K. L., Rivlin, T., Schneider, K., Sesboüé, M., Shamberger, K., Silverman, J., Wolfe, K., Zhu, K., and Caldeira, K.: Reversal of ocean acidification enhances net coral reef calcification, *Nature*, 531, 362–365, <https://doi.org/10.1038/nature17155>, 2016.
- Aller, R. C.: Carbonate Dissolution in Nearshore Terrigenous Muds: The Role of Physical and Biological Reworking, *J Geol*, 90, 79–95, <https://doi.org/10.1086/628652>, 1982.
- Archer, D., Kheshgi, H., and Maier-Reimer, E.: Dynamics of fossil fuel CO_2 neutralization by marine CaCO_3 , *Global Biogeochem Cycles*, 12, 259–276, <https://doi.org/10.1029/98GB00744>, 1998.
- Bach, L. T., Gill, S. J., Rickaby, R. E. M., Gore, S., and Renforth, P.: CO_2 Removal With Enhanced Weathering and Ocean Alkalinity Enhancement: Potential Risks and Co-benefits for Marine Pelagic Ecosystems, *Frontiers in Climate*, 1, 1–21, <https://doi.org/10.3389/fclim.2019.00007>, 2019.
- Caserini, S., Storni, N., and Grosso, M.: The Availability of Limestone and Other Raw Materials for Ocean Alkalinity Enhancement, *Global Biogeochem Cycles*, 36, <https://doi.org/10.1029/2021GB007246>, 2022.
- Dickson, A. G., Afghan, J. D., and Anderson, G. C.: Reference materials for oceanic CO_2 analysis: a method for the certification of total alkalinity, *Mar Chem*, 80, 185–197, [https://doi.org/10.1016/S0304-4203\(02\)00133-0](https://doi.org/10.1016/S0304-4203(02)00133-0), 2003.
- Dickson, A. G., Sabine, C. L., and Christian, J. R.: Guide to Best Practices for Ocean CO_2 Measurements, *PICES Spec.*, PICES, Sidney, 2007.
- Eisaman, M. D., Rivest, J. L. B., Karnitz, S. D., Lannoy, C. De, Jose, A., Devaul, R. W., and Hannun, K.: International Journal of Greenhouse Gas Control Indirect ocean capture of atmospheric CO_2 : Part II . Understanding the cost of negative emissions, *International Journal of Greenhouse Gas Control*, 70, 254–261, <https://doi.org/10.1016/j.ijggc.2018.02.020>, 2018.
- Eisaman, M. D., Geilert, S., Renforth, P., Bastianini, L., Campbell, J., Dale, A. W., Foteinis, S., Grasse, P., Hawrot, O., Löscher, C. R., Rau, G. H., and Rønning, J.: Chapter 3: Assessing the technical aspects of OAE approaches, in: *Guide for best practices in Ocean Alkalinity Enhancement*, 2023a.
- Fakhraee, M., Planavsky, N. J., and Reinhard, C. T.: Ocean alkalinity enhancement through restoration of blue carbon ecosystems, *Nat Sustain*, <https://doi.org/10.1038/s41893-023-01128-2>, 2023.
- Feng, E. Y., Koeve, W., Keller, D. P., and Oschlies, A.: Model-Based Assessment of the CO_2 Sequestration Potential of Coastal Ocean Alkalinization, *Earths Future*, 5, 1252–1266, <https://doi.org/10.1002/ef2.273>, 2017.

903 Ferderer, A., Chase, Z., Kennedy, F., Schulz, K. G., and Bach, L. T.: Assessing the influence of
 904 ocean alkalinity enhancement on a coastal phytoplankton community, *Biogeosciences*, 19,
 905 5375–5399, <https://doi.org/10.5194/bg-19-5375-2022>, 2022.
 906 Flipkens, G., Fuhr, M., Meysman, F. J. R., Town, R. M., and Blust, R.: Enhanced olivine
 907 dissolution in seawater through continuous grain collisions, *Geochim Cosmochim Acta*, 359,
 908 84–99, <https://doi.org/10.1016/j.gca.2023.09.002>, 2023.
 909 Fuhr, M., Geilert, S., Schmidt, M., Liebetrau, V., Vogt, C., Ledwig, B., and Wallmann, K.:
 910 Kinetics of Olivine Weathering in Seawater: An Experimental Study, *Frontiers in Climate*, 4,
 911 1–20, <https://doi.org/10.3389/fclim.2022.831587>, 2022.
 912 Gattuso, J.-P., Epitalon, J.-M., Lavigne, H., and Orr, J.: Seacarb: seawater carbonate
 913 chemistry with R. R package version 3.0, 2021.
 914 Hangx, S. J. T. and Spiers, C. J.: Coastal spreading of olivine to control atmospheric CO₂
 915 concentrations: A critical analysis of viability, *International Journal of Greenhouse Gas*
 916 *Control*, 3, 757–767, <https://doi.org/10.1016/j.ijggc.2009.07.001>, 2009.
 917 Hansen, H. P. and Koroleff, F.: Determination of nutrients, in: *Methods of Seawater Analysis*,
 918 edited by: Grasshoff, K., Kremling, K., and Ehrhardt, M., Wiley-VCH, Weinheim, 159–226,
 919 1999.
 920 Hartmann, J., West, a J., Renforth, P., Köhler, P., De La Rocha, C. L., Wolf-Gladrow, D. A,
 921 Dürr, H. H., and Scheffran, J.: Enhanced chemical weathering as a geoengineering strategy to
 922 reduce atmospheric carbon dioxide, supply nutrients, and mitigate ocean acidification,
 923 *Reviews of Geophysics*, 51, 113–149, <https://doi.org/10.1002/rog.20004.1>.Institute, 2013.
 924 Hartmann, J., Suitner, N., Lim, C., Schneider, J., Marín-Samper, L., Arístegui, J., Renforth, P.,
 925 Taucher, J., and Riebesell, U.: Stability of alkalinity in ocean alkalinity enhancement (OAE)
 926 approaches - consequences for durability of CO₂ storage, *Biogeosciences*, 20, 781–802,
 927 <https://doi.org/10.5194/bg-20-781-2023>, 2023.
 928 Harvey, L. D. D.: Mitigating the atmospheric CO₂ increase and ocean acidification by adding
 929 limestone powder to upwelling regions, *J Geophys Res Oceans*, 113, 1–21,
 930 <https://doi.org/10.1029/2007JC004373>, 2008.
 931 Havukainen, M., Waldén, P., and Kahiluoto, H.: Clean Development Mechanism, in:
 932 *Encyclopedia of Sustainable Management*, edited by: Idowu, S. O., Springer Nature
 933 Switzerland, 1–5, <https://doi.org/10.1016/B978-0-12-375067-9.00127-3>, 2022.
 934 He, J. and Tyka, M. D.: Limits and CO₂ equilibration of near-coast alkalinity enhancement,
 935 *Biogeosciences*, 20, 27–43, <https://doi.org/10.5194/bg-20-27-2023>, 2023.
 936 Humphreys, M. P., Gregor, L., Pierrot, D., van Heuven, S. M. A. C., Lewis, E. R., and Wallace,
 937 D. W. R.: PyCO₂SYs: marine carbonate system calculations in Python,
 938 <https://doi.org/10.5281/zenodo.3744275>, 2020.
 939 Keller, D. P., Lenton, A., Littleton, E. W., Oschlies, A., Scott, V., and Vaughan, N. E.: The
 940 Effects of Carbon Dioxide Removal on the Carbon Cycle, *Curr Clim Change Rep*, 4, 250–265,
 941 <https://doi.org/10.1007/s40641-018-0104-3>, 2018.
 942 Krumins, V., Gehlen, M., Arndt, S., Van Cappellen, P., and Regnier, P.: Dissolved inorganic
 943 carbon and alkalinity fluxes from coastal marine sediments: Model estimates for different
 944 shelf environments and sensitivity to global change, *Biogeosciences*, 10, 371–398,
 945 <https://doi.org/10.5194/bg-10-371-2013>, 2013.
 946 de Lannoy, C. F., Eisaman, M. D., Jose, A., Karnitz, S. D., DeVaul, R. W., Hannun, K., and
 947 Rivest, J. L. B.: Indirect ocean capture of atmospheric CO₂: Part I. Prototype of a negative
 948 emissions technology, *International Journal of Greenhouse Gas Control*, 70, 243–253,
 949 <https://doi.org/10.1016/j.ijggc.2017.10.007>, 2018.

950 Lezaun, J.: Hugging the Shore: Tackling Marine Carbon Dioxide Removal as a Local
 951 Governance Problem, *Frontiers in Climate*, 3, 1–6,
 952 <https://doi.org/10.3389/fclim.2021.684063>, 2021.
 953 Liu, Y., Jiao, J. J., Liang, W., Santos, I. R., Kuang, X., and Robinson, C. E.: Inorganic carbon and
 954 alkalinity biogeochemistry and fluxes in an intertidal beach aquifer: Implications for ocean
 955 acidification, *J Hydrol (Amst)*, 595, 126036, <https://doi.org/10.1016/j.jhydrol.2021.126036>,
 956 2021.
 957 Lueker, T. J., Dickson, A. G., and Keeling, C. D.: Ocean pCO₂ calculated from dissolved
 958 inorganic carbon, alkalinity, and equations for K₁ and K₂: Validation based on laboratory
 959 measurements of CO₂ in gas and seawater at equilibrium, *Mar Chem*, 70, 105–119,
 960 [https://doi.org/10.1016/S0304-4203\(00\)00022-0](https://doi.org/10.1016/S0304-4203(00)00022-0), 2000.
 961 Lunstrum, A. and Berelson, W.: CaCO₃ dissolution in carbonate-poor shelf sands increases
 962 with ocean acidification and porewater residence time, *Geochim Cosmochim Acta*, 329,
 963 168–184, <https://doi.org/10.1016/j.gca.2022.04.031>, 2022.
 964 Meysman, F. J. R. and Montserrat, F.: Negative CO₂ emissions via enhanced silicate
 965 weathering in coastal environments, *Biol Lett*, 13, 20160905,
 966 <https://doi.org/10.1098/rsbl.2016.0905>, 2017.
 967 Michaelowa, A., Hermwille, L., Obergassel, W., and Butzengeiger, S.: Additionality revisited:
 968 guarding the integrity of market mechanisms under the Paris Agreement, *Climate Policy*, 19,
 969 1211–1224, <https://doi.org/10.1080/14693062.2019.1628695>, 2019.
 970 Middelburg, J. J., Soetaert, K., and Hagens, M.: Ocean Alkalinity, Buffering and
 971 Biogeochemical Processes, *Reviews of Geophysics*, 58,
 972 <https://doi.org/10.1029/2019RG000681>, 2020.
 973 Milliman, J. D., Troy, P. J., Balch, W. M., Adams, a. K., Li, Y.-H., and Mackenzie, F. T.:
 974 Biologically mediated dissolution of calcium carbonate above the chemical lysocline?, *Deep*
 975 *Sea Research Part I: Oceanographic Research Papers*, 46, 1653–1669,
 976 [https://doi.org/10.1016/S0967-0637\(99\)00034-5](https://doi.org/10.1016/S0967-0637(99)00034-5), 1999.
 977 Mongin, M., Baird, M. E., Lenton, A., Neill, C., and Akl, J.: Reversing ocean acidification along
 978 the Great Barrier Reef using alkalinity injection, *Environmental Research Letters*, 16,
 979 <https://doi.org/10.1088/1748-9326/ac002d>, 2021.
 980 Montserrat, F., Renforth, P., Hartmann, J., Leermakers, M., Knops, P., and Meysman, F. J. R.:
 981 Olivine Dissolution in Seawater: Implications for CO₂ Sequestration through Enhanced
 982 Weathering in Coastal Environments, *Environ Sci Technol*, 51, 3960–3972,
 983 <https://doi.org/10.1021/acs.est.6b05942>, 2017.
 984 Moras, C. A., Bach, L. T., Cyronak, T., Joannes-Boyau, R., and Schulz, K. G.: Ocean alkalinity
 985 enhancement - avoiding runaway CaCO₃ precipitation during quick and hydrated lime
 986 dissolution, *Biogeosciences*, 19, 3537–3557, <https://doi.org/10.5194/bg-19-3537-2022>,
 987 2022.
 988 Morse, J. W., Zullig, J. J., Bernstein, L. D., Millero, F. J., Milne, P., Mucci, A., and Choppin, G.
 989 R.: Chemistry of calcium carbonate-rich shallow water sediments in the Bahamas., *Am J Sci*,
 990 285, 147–185, <https://doi.org/10.2475/ajs.285.2.147>, 1985.
 991 Morse, J. W., Gledhill, D. K., and Millero, F. J.: CaCO₃ precipitation kinetics in waters from
 992 the great Bahama bank: Implications for the relationship between bank hydrochemistry and
 993 whittings, *Geochim Cosmochim Acta*, 67, 2819–2826, [https://doi.org/10.1016/S0016-7037\(03\)00103-0](https://doi.org/10.1016/S0016-7037(03)00103-0), 2003.
 994 Mucci, A.: The solubility of calcite and aragonite in seawater at various salinities,
 995 temperatures, and one atmosphere total pressure, *Am J Sci*, 283, 780–799, 1983.

997 Nemet, G. F., Callaghan, M. W., Creutzig, F., Fuss, S., Hartmann, J., Hilaire, J., Lamb, W. F.,
 998 Minx, J. C., Rogers, S., and Smith, P.: Negative emissions — Part 3: Innovation and upscaling,
 999 *Environmental Research Letters*, 13, 06300, 2018.
 1000 Oelkers, E. H., Declercq, J., Saldi, G. D., Gislason, S. R., and Schott, J.: Olivine dissolution
 1001 rates: A critical review, *Chem Geol*, 500, 1–19,
 1002 <https://doi.org/10.1016/j.chemgeo.2018.10.008>, 2018.
 1003 Perkins, A. K., Santos, I. R., Rose, A. L., Schulz, K. G., Grossart, H. P., Eyre, B. D., Kelaher, B. P.,
 1004 and Oakes, J. M.: Production of dissolved carbon and alkalinity during macroalgal wrack
 1005 degradation on beaches: a mesocosm experiment with implications for blue carbon,
 1006 *Biogeochemistry*, 160, 159–175, <https://doi.org/10.1007/s10533-022-00946-4>, 2022.
 1007 Rau, G. H. and Caldeira, K.: Enhanced carbonate dissolution: A means of sequestering waste
 1008 CO₂ as ocean bicarbonate, *Energy Convers Manag*, 40, 1803–1813,
 1009 [https://doi.org/10.1016/S0196-8904\(99\)00071-0](https://doi.org/10.1016/S0196-8904(99)00071-0), 1999.
 1010 Reckhardt, A., Beck, M., Seidel, M., Riedel, T., Wehrmann, A., Bartholomä, A., Schnetger, B.,
 1011 Dittmar, T., and Brumsack, H. J.: Carbon, nutrient and trace metal cycling in sandy
 1012 sediments: A comparison of high-energy beaches and backbarrier tidal flats, *Estuar Coast*
 1013 *Shelf Sci*, 159, 1–14, <https://doi.org/10.1016/j.ecss.2015.03.025>, 2015.
 1014 Renforth, P.: The negative emission potential of alkaline materials, *Nat Commun*, 10,
 1015 <https://doi.org/10.1038/s41467-019-09475-5>, 2019.
 1016 Renforth, P. and Henderson, G.: Assessing ocean alkalinity for carbon sequestration,
 1017 *Reviews of Geophysics*, 55, 636–674, <https://doi.org/10.1002/2016RG000533>, 2017.
 1018 Renforth, P., Baltruschat, S., Peterson, K., Mihailova, B. D., and Hartmann, J.: Using ikaite
 1019 and other hydrated carbonate minerals to increase ocean alkalinity for carbon dioxide
 1020 removal and environmental remediation, *Joule*, 6, 2674–2679,
 1021 <https://doi.org/10.1016/j.joule.2022.11.001>, 2022a.
 1022 Renforth, P., Baltruschat, S., Peterson, K., Mihailova, B. D., and Hartmann, J.: Using ikaite
 1023 and other hydrated carbonate minerals to increase ocean alkalinity for carbon dioxide
 1024 removal and environmental remediation, *Joule*, 6, 2674–2679,
 1025 <https://doi.org/10.1016/j.joule.2022.11.001>, 2022b.
 1026 Saderne, V., Fusi, M., Thomson, T., Dunne, A., Mahmud, F., Roth, F., Carvalho, S., and
 1027 Duarte, C. M.: Total alkalinity production in a mangrove ecosystem reveals an overlooked
 1028 Blue Carbon component, *Limnol Oceanogr Lett*, 6, 61–67,
 1029 <https://doi.org/10.1002/lol2.10170>, 2021.
 1030 Schuiling, R. D. and de Boer, P. L.: Coastal spreading of olivine to control atmospheric CO₂
 1031 concentrations: A critical analysis of viability. Comment: Nature and laboratory models are
 1032 different, *International Journal of Greenhouse Gas Control*, 4, 855–856,
 1033 <https://doi.org/10.1016/j.ijggc.2010.04.012>, 2010.
 1034 Schuiling, R. D. and Krijgsman, P.: Enhanced weathering: An effective and cheap tool to
 1035 sequester CO₂, *Clim Change*, 74, 349–354, <https://doi.org/10.1007/s10584-005-3485-y>,
 1036 2006.
 1037 Schulz, K. G., Bach, L. T., and Dickson, A. G.: Seawater carbonate system considerations for
 1038 ocean alkalinity enhancement research, *Guide for best practices in Ocean Alkalinity*
 1039 *Enhancement*, 2023.
 1040 Subhas, A. V., Dong, S., Naviaux, J. D., Rollins, N. E., Ziveri, P., Gray, W., Rae, J. W. B., Liu, X.,
 1041 Byrne, R. H., Chen, S., Moore, C., Martell-Bonet, L., Steiner, Z., Antler, G., Hu, H., Lunstrum,
 1042 A., Hou, Y., Kemnitz, N., Stutsman, J., Pallacks, S., Dugenne, M., Quay, P. D., Berelson, W. M.,

1043 and Adkins, J. F.: Shallow Calcium Carbonate Cycling in the North Pacific Ocean, *Global*
 1044 *Biogeochem Cycles*, 36, 1–22, <https://doi.org/10.1029/2022GB007388>, 2022.
 1045 Sulpis, O., Jeansson, E., Dinauer, A., Lauvset, S. K., and Middelburg, J. J.: Calcium carbonate
 1046 dissolution patterns in the ocean, *Nat Geosci*, 14, 423–428, [https://doi.org/10.1038/s41561-](https://doi.org/10.1038/s41561-021-00743-y)
 1047 [021-00743-y](https://doi.org/10.1038/s41561-021-00743-y), 2021.
 1048 Sulpis, O., Agrawal, P., Wolthers, M., Munhoven, G., Walker, M., and Middelburg, J. J.:
 1049 Aragonite dissolution protects calcite at the seafloor, *Nat Commun*, 13, 1–8,
 1050 <https://doi.org/10.1038/s41467-022-28711-z>, 2022.
 1051 Torres, M. E., Hong, W. L., Solomon, E. A., Milliken, K., Kim, J. H., Sample, J. C., Teichert, B.
 1052 M. A., and Wallmann, K.: Silicate weathering in anoxic marine sediment as a requirement for
 1053 authigenic carbonate burial, *Earth Sci Rev*, 200, 102960,
 1054 <https://doi.org/10.1016/j.earscirev.2019.102960>, 2020.
 1055 Tyka, M. D., Van Arsdale, C., and Platt, J. C.: CO₂ capture by pumping surface acidity to the
 1056 deep ocean, *Energy Environ Sci*, 15, 786–798, <https://doi.org/10.1039/d1ee01532j>, 2022.
 1057 Wallmann, K., Diesing, M., Scholz, F., Rehder, G., Dale, A. W., Fuhr, M., and Suess, E.: Erosion
 1058 of carbonate-bearing sedimentary rocks may close the alkalinity budget of the Baltic Sea
 1059 and support atmospheric CO₂ uptake in coastal seas, *Front Mar Sci*, 9, 1–15,
 1060 <https://doi.org/10.3389/fmars.2022.968069>, 2022.
 1061 Zhong, S. and Mucci, A.: Calcite and aragonite precipitation from seawater solutions of
 1062 various salinities: Precipitation rates and overgrowth compositions, *Chem Geol*, 78, 283–
 1063 299, [https://doi.org/10.1016/0009-2541\(89\)90064-8](https://doi.org/10.1016/0009-2541(89)90064-8), 1989.
 1064